Institut für Kernphysik
Schloßgartenstraße 9
64289 Darmstadt

TECHNISCHE UNIVERSITÄT DARMSTADT

Hadronic Mass Spectrum and Thermodynamics in the MIT Bag Model

Massenspektrum und Thermodynamik von Hadronen im MIT Bag Model

Bachelor-Thesis

Jan Lücker

Supervision: Prof. Dr. Jochen Wambach
Dr. Dominik Nickel

November 2007

Zusammenfassung

In dieser Arbeit wird das Spektrum leichter Hadronen in der Quantenchromodynamik (QCD) mithilfe des MIT Bag Model untersucht, ein Modell das 1974 am MIT entwickelt wurde. Mit diesem Modell werden die Massen leichter Hadronen, deren radiale Anregungen und ein asymptotisches Massenspektrum bestimmt. Die Ergebnisse dieser Untersuchung werden benutzt um ein Gas von Hadronen zu beschreiben. Dieses Gas wird mit zwei Modellen beschrieben, als ein Quantengas von punktförmigen Teilchen und im Compressible Bag Model, welches das Volumen der Hadronen berücksichtigt. Die Eigenschaften eines Hadronengases in diesen Modellen wird mit den Ergebnissen von Lattice QCD Berechnungen verglichen. Dabei ist der Phasenübergang in ein Quark-Gluonen-Plasma von besonderem Interesse.

Abstract

In this work the spectrum of light hadrons in quantum chromodynamics (QCD) is investigated by using the MIT Bag Model, a model that has been developed in 1974 at the MIT. This model is used to calculate the masses of light hadrons, their radial excitations and an asymptotic mass spectrum. The results of this investigation are used for the description of a gas of hadrons. This gas is described by using two models, as a quantum gas of point-like particles and in the compressible bag model, which incorporates the volume of the hadrons. The properties of a hadron gas in these models are compared to the results of lattice QCD calculations. The phase transition to a quark-gluon plasma is of special interest here.

Contents

1 Introduction

The theory of quantum chromodynamics (QCD) describes the interactions of quarks and gluons. A bound state of quarks in the QCD is called a hadron, which can not be left by its valence quarks. In 1974 Chodos, Jaffe, Johnson, Thorn and Weisskopf from the Massachusetts Institute of Technology introduced a new model of hadrons, see Ref. [2], in which hadrons are treated as so-called 'bags'. This model has been used in 1975 by DeGrand, Jaffe, Johnson and Kiskis to calculate the spectrum of light, ground-state hadrons, see Ref. [3]. To describe the state of quarks inside a hadron the MIT Bag Model takes the QCD vacuum to be a medium in which the quarks can not exist. They are bound inside a region of space, a so-called 'bag', in which they are treated as free particles. Their kinetic energy and some correction terms are used to determine the hadron mass. This model leads to a considerably good agreement with the experimental data, and is presented here.

After some hadron masses are calculated, the thermodynamic properties of a gas of hadrons are investigated. The most interesting property of such a gas is the phase transition to a quark-gluon plasma. In a quark-gluon plasma the quarks and gluons, which are confined in hadronic matter, are deconfined. This state of matter is believed to be produced in collider experiments of high energies, and is a subject of thorough investigations. To describe a gas of hadrons, two models are used:

- An ideal quantum gas. The limits of this model will be reached when the phase diagram of QCD is calculated.
- The compressible bag model, an approach in which the volume of the bags is taken into account. This will result in a more reasonably phase diagram.

As no experimental data exist to date, the results from the bag model are compared to lattice QCD calculations.

1.1 Units

Natural units are used here: $\hbar = c = k_B = 1$. With $\hbar c = 197.3\text{MeVfm}$ and $k_B = 8,617 \cdot 10^{-11} \frac{\text{MeV}}{\text{K}}$ the conversions for length and temperature are $1\text{fm} = 5.068\text{GeV}^{-1}$ and $1\text{K} = 8,617 \cdot 10^{-11}\text{MeV}$.

2 The MIT Bag Model

As the properties of hadrons could not yet be calculated with full QCD, several models have been developed to describe a hadron. A relatively simple one is the bag model. The hadron is described as a cavity to which the quarks are confined, and which they can not leave. The MIT Bag Model explains the stability of this cavity by introducing the universal bag constant B as the inward vacuum pressure. Now the radius of the bag is determined by the equilibrium of B and the outward pressure created by the valence quarks.

To calculate the mass of a hadron the Dirac equation for one quark is solved inside a spherical cavity of radius r with wave function ψ as solution. Outside the bag, the wave function is zero. (See Fig. 2.1 as an illustration.) The scalar $\bar{\psi}\psi$ has to vanish on the surface of the bag, a consequence of the bag Lagrangian. This boundary condition determines the kinetic energy of the quarks. Several correction energy terms are introduced: Zero point fluctuations and center of mass movement are summarized in a parameter Z_0 which has to be fitted to experimental values. The quark-gluon interactions are calculated to the lowest order in the coupling constant α_S. The sum over these energies and the energy contributed by the bag constant is identified as the mass of the hadron, which is a function of the bag radius: $M(r)$. Now $M(r)$ is minimized with respect to the radius. This determines the hadron radius R, and therefore the resulting mass $M(R)$. The minimization condition is equivalent to the equilibrium of outside and inside pressure on the bag surface, and therefore to the stability of the bag.

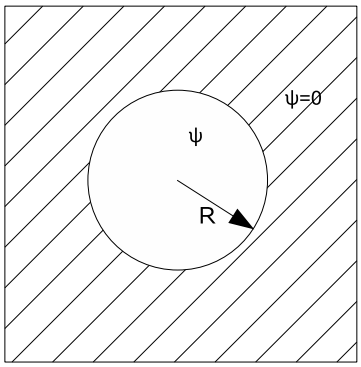

Figure 2.1: Illustration of the bag model: The quark wave function ψ is non-zero inside a spherical cavity, surrounded by QCD vacuum in which the wave function is $\psi = 0$.

2.1 The bag Lagrangian

To start with, the bag Lagrangian for a spherical and static bag of radius R is written down as

$$\mathcal{L} = \left\{\bar{\psi}\left(i\gamma_\mu\partial^\mu - m\right)\psi - B\right\}\Theta(R-r) - \bar{\psi}\psi\delta(R-r). \tag{2.1}$$

Here Θ is the Heaviside step function and δ the Dirac delta function. They are related through

$$\partial_\mu \Theta(r) = n_\mu \delta(r),$$

where $(n^\mu) = (0, \vec{e}_r)$ is the unit vector perpendicular to the bag surface. Inside the bag ($r < R$), the bag Lagrangian is just the Lagrangian for a free fermion of mass m. Also the bag constant B is subtracted here as it contributes to the energy density, but with no effect on the equations of motion. On the bag surface ($r = R$) the term $\bar{\psi}\psi$ in the Lagrangian will give the boundary condition.

Now according to Hamilton's principle the action of the system is minimized, which leads to the Euler-Lagrange equations

$$\partial_\mu \frac{\partial \mathcal{L}}{\partial(\partial_\mu \psi)} - \frac{\partial \mathcal{L}}{\partial \psi} = 0. \tag{2.2}$$

Deriving these equations from Eq. (2.1) leads to the Dirac equation

$$(i\gamma_\mu \partial^\mu - m)\,\psi = 0 \tag{2.3}$$

inside the bag. This equation will be solved in the following section. On the bag surface the Euler-Lagrange equations lead to

$$-i\vec{\gamma}\vec{e}_r\psi = \psi,$$

which is the boundary condition. It can also be written as $i\bar{\psi}\vec{\gamma}\vec{e}_r = \bar{\psi}$. Now $\bar{\psi}\psi$ is constructed from both forms, and one gets

$$\bar{\psi}\psi = i\bar{\psi}\vec{\gamma}\vec{e}_r\psi = -i\bar{\psi}\vec{\gamma}\vec{e}_r\psi = 0. \tag{2.4}$$

This is the boundary condition that will be used to determine the momentum of a quark inside the bag.

A word about chiral symmetry is in order here. The Lagrangian of a free massless quark is chirally symmetric, but the symmetry is broken when a quark mass is introduced. So the symmetry breaking term is $m\bar{\psi}\psi$. In the bag Lagrangian the term $\delta(R-r)\bar{\psi}\psi$ does the same, even for vanishing quark masses. In a chirally symmetric theory massless pions are expected if the symmetry is dynamically broken. If the symmetry is explicitely broken on the level of the Langrangian, as it is here, the pions should be massive.

2.2 Calculation of hadron masses

In this section the masses of light hadrons will be calculated in the way described by DeGrand in Ref. [3]. The mass of a hadron is composited in the following way:

$$M = E_{kin} + E_0 + E_{mag} + E_{el} + E_{vol}.$$

The contributions in this formula are

- the kinetic energy of the quarks E_{kin},
- the correction energy E_0 which includes effects not calculated here,
- the magnetic and electric interaction energies E_{mag} and E_{el},
- and the volume energy E_{vol} given by the bag constant.

These energies will now be discussed.

2.2.1 The kinetic energy of a fermion in a spherical cavity

As shown above, the Lagrangian of one quark leads to the Dirac equation inside the bag, which is a spherical cavity here:

$$(i\gamma_\mu \partial^\mu - m)\,\psi = 0. \tag{2.5}$$

Here, ψ is the four-component wave function, m the mass of the quark, γ_μ are the γ-matrices and $\partial^\mu = \left(\frac{\partial}{\partial t}, -\vec{\nabla}\right)$. Now the Dirac representation of the γ-matrices is chosen:

$$\gamma_0 = \begin{pmatrix} 1 & 0 \\ 0 & -1 \end{pmatrix}, \quad \gamma_i = \begin{pmatrix} 0 & \sigma_i \\ -\sigma_i & 0 \end{pmatrix},$$

where σ_i are the Pauli matrices. This allows for ψ to be written as two two-component spinors for particle and anti-particle. Together with the stationary case as solution for the time dependence, the wave function becomes:

$$\psi(\vec{x}, t) = \begin{pmatrix} \phi(\vec{x}) \\ \chi(\vec{x}) \end{pmatrix} e^{-iEt}.$$

With $\phi(\vec{x})$ and $\chi(\vec{x})$ for particle and antiparticle, respectively. The energy is $E = \sqrt{m^2 + p^2}$. The Dirac equation is now written as two coupled equations of ϕ and χ by using the Dirac representation of the gamma matrices. With these Eq. (2.5) becomes:

$$\begin{aligned} (\vec{\sigma}\vec{p})\,\chi + m\phi &= E\phi, & (2.6)\\ (\vec{\sigma}\vec{p})\,\phi - m\chi &= E\chi. & (2.7) \end{aligned}$$

These coupled equations can easily be decoupled by solving e.g. Eq. (2.6) for ϕ and inserting it into Eq. (2.7). Now the momentum is written in its operator representation $\vec{p} = -i\vec{\nabla}$, and the identity $(\vec{\sigma}\vec{a})^2 = \vec{a}^2$ is used to get the decoupled equations

$$\begin{aligned} -\Delta\phi &= \left(E^2 - m^2\right)\phi, & (2.8)\\ -\Delta\chi &= \left(E^2 - m^2\right)\chi, & (2.9) \end{aligned}$$

where $\Delta = \vec{\nabla}^2$. The solutions for these equations are well known, as they appear for example in a similar form in the Schrödinger description of the hydrogen atom. And just as in that case, the angular part of the Laplace operator can be separated here. It is solved by spherical harmonic functions but with the difference that here, unlike the case of the Schrödinger equation, the spin has to be taken care of. The solution looks like

$$\begin{aligned} \phi(\vec{r}) &= g(r)\mathcal{Y}^{j_3}_{j,l}(\theta,\varphi), & (2.10)\\ \chi(\vec{r}) &= f(r)\mathcal{Y}^{j_3}_{j,l'}(\theta,\varphi), & (2.11) \end{aligned}$$

where $\mathcal{Y}^{j_3}_{j,l}$ is a spinor in space representation for the total angular momentum $\vec{J} = \vec{L} + \frac{1}{2}\vec{\sigma}$ with quantum number j. The spinor is written as

$$\mathcal{Y}^{j_3}_{j,l} = \begin{pmatrix} \left(l\,\frac{1}{2}\,j_3 - \frac{1}{2}\,\frac{1}{2}\middle|\,j\,j_3\right) Y_l^{j_3 - \frac{1}{2}} \\ \left(l\,\frac{1}{2}\,j_3 + \frac{1}{2}\,-\frac{1}{2}\middle|\,j\,j_3\right) Y_l^{j_3 + \frac{1}{2}} \end{pmatrix},$$

where $(l\, l_3\, s\, m_s | j\, j_3)$ are the Clebsch-Gordan coefficients, which transform the basis of $\vec{L}$ with quantum numbers l and l_3 and $\frac{1}{2}\vec{\sigma}$ with quantum numbers $s = \frac{1}{2}$ and m_s to the basis of the total spin $\vec{J}$ with quantum numbers j and j_3. The quantum numbers of particle and antiparticle, l and l', are related through the quantum number κ, defined as the eigenvalues of

$$K = \beta \left(\vec{\Sigma} \cdot \vec{l} + 1 \right).$$

This leads to

$$l = \begin{cases} \kappa, & \text{for } \kappa > 0 \\ -(\kappa + 1), & \text{for } \kappa < 0 \end{cases} \tag{2.12}$$

$$l' = \begin{cases} \kappa - 1, & \text{for } \kappa > 0 \\ -\kappa, & \text{for } \kappa < 0 \end{cases} \tag{2.13}$$

After the separation of the angular dependencies, the radial components of Eqs. (2.8) and (2.9) are

$$0 = r^2 \frac{d^2 f}{dr^2} + 2r \frac{df}{dr} + \left[r^2 p^2 - l(l+1) \right] f, \tag{2.14}$$

$$0 = r^2 \frac{d^2 g}{dr^2} + 2r \frac{dg}{dr} + \left[r^2 p^2 - l'(l'+1) \right] g. \tag{2.15}$$

This form of differential equation is again well known, the solutions are spherical Bessel functions. With them, the Dirac equation is solved and the radial components of Eqs. (2.10) and (2.11) are:

$$\begin{aligned} f(r) &= N \sqrt{\frac{E+m}{E}} j_l(pr), \\ g(r) &= N \sqrt{\frac{E-m}{E}} j_{l'}(pr). \end{aligned}$$

Where N is the normalization constant. It is now easy to show that the density $\psi^\dagger \psi$ is only radial symmetric if $l = 0$ and $l' = 1$ (which means $\kappa = -1$). This has to be fulfilled, as the basic assumption was that the pressure is in equilibrium on the whole surface of the bag. If the density was not radial symmetric, the bag would not be spherical anymore.

$$\psi^\dagger \psi = \left(f^2 \left(\mathcal{Y}^{j_3}_{j,l'} \right)^\dagger \mathcal{Y}^{j_3}_{j,l'} + g^2 \left(\mathcal{Y}^{j_3}_{j,l} \right)^\dagger \mathcal{Y}^{j_3}_{j,l} \right) \tag{2.16}$$

Now using that unity can be written as $1 = (\vec{\sigma}\vec{e}_r)\,(\vec{\sigma}\vec{e}_r)$ and that (see for example Ref. [4]) $(\vec{\sigma}\vec{e}_r)\,\mathcal{Y}^{j_3}_{j,l'} = -\mathcal{Y}^{j_3}_{j,l}$ Eq. (2.16) becomes

$$\psi^\dagger \psi = \left(f^2 + g^2 \right) \left(\mathcal{Y}^{j_3}_{j,l} \right)^\dagger \mathcal{Y}^{j_3}_{j,l}.$$

As the only spherical harmonic function that is independent of the angle is Y^0_0, the claim is proven. Recalling Eq. (2.4), $\bar{\psi}\psi\big|_{r=R} = 0$, the boundary condition is

$$\bar{\psi}\psi\big|_R = \psi^\dagger \gamma_0 \psi \Big|_R = (g\, f) \begin{pmatrix} g \\ -f \end{pmatrix} \Bigg|_R = \left(g^2 - f^2 \right)\big|_R \stackrel{!}{=} 0.$$

It follows the final equation to calculate the momentum as a function of radius:

$$(E+m)\cdot j_0^2(pR) = (E-m)\cdot j_1^2(pR), \tag{2.17}$$

where the first and second spherical Bessel functions are

$$j_0(x) = \frac{\sin(x)}{x}, \tag{2.18}$$

$$j_1(x) = \frac{\sin(x)}{x^2} - \frac{\cos(x)}{x}. \tag{2.19}$$

This equation has to be solved numerically. The solution is $p(R)$, and the kinetic energy of quark i inside the bag is written as

$$E_{kin,i}(R) = \sqrt{p_i^2(R) + m^2}. \tag{2.20}$$

With the sum of the kinetic energies of the quarks in a hadron and the volume term, the mass of a hadron could now be calculated to a first approximation. But some correction and interaction terms will also be added.

2.2.2 The correction term E_0

The correction energy

$$E_0 = Z_0/r \tag{2.21}$$

contains contributions that are difficult or impossible to calculate. In Ref. [3], an estimate for zero-point energies is given, resulting in a $Z_0 \approx -2$. The correction term also includes center of mass corrections, which are approximated in some works, for example in Ref. [5]. Here Z_0 is treated as an open parameter of the bag model and will be fitted together with the bag constant and the coupling constant to hadron masses later.

2.2.3 Quark interaction energy

Figure 2.2: Lowest order interaction Feynman diagrams. The straight lines are quark propagators and the jagged lines are gluon propagators.

The gluon exchange and the quark self energy terms, as shown in Fig. 2.2, are calculated here. To the lowest order in $\alpha_S = \frac{g^2}{4\pi}$, where g is the color charge in QCD, the problem reduces to solving the electromagnetic case with the boundary conditions

$$\vec{e}_r \times \vec{B}^a\Big|_{r=R} = 0, \tag{2.22}$$

$$\vec{e}_r \cdot \vec{E}^a\Big|_{r=R} = 0, \tag{2.23}$$

where $a \in \{1, 8\}$ denotes the color index. The electric and magnetic interaction energies are then

$$E_{mag} = -\frac{1}{2}g^2 \sum_a \int_{bag} d^3x \left(\vec{B}^a(\vec{x})\right)^2, \tag{2.24}$$

$$E_{el} = \frac{1}{2}g^2 \sum_a \int_{bag} d^3x \left(\vec{E}^a(\vec{x})\right)^2. \tag{2.25}$$

See Ref. [3] for more information. A short presentation of the calculation follows now.

Magnetic interaction

To calculate Eq. (2.24) Maxwell's equations are used to determine the magnetic field of the i-th quark:

$$\vec{\nabla} \times \vec{B}_i^a = \vec{j}_i^a, \tag{2.26}$$

$$\vec{\nabla} \vec{B}_i^a = 0, \tag{2.27}$$

inside the bag. The vector current is $\vec{j}_i^a = \bar{\psi}_i \vec{\gamma} \lambda^a \psi_i$, where the Gell-Mann matrices λ^a are generators for the $SU(3)$ symmetry group. From these equations, the magnetic interaction energy for a hadron in the ground state becomes

$$E_{mag} = 2\alpha_S \lambda \sum_{i>j} \langle \vec{\sigma}_i \vec{\sigma}_j \rangle \frac{\mu(m_i, R) \cdot \mu(m_j, R)}{R^3} I(m_i, m_j, R), \tag{2.28}$$

with $\lambda = 2$ for mesons and $\lambda = 1$ for baryons. The magnetic moment of one quark is

$$\mu(m_i, R) = \int d^3x \frac{1}{2}\vec{r} \times \left(\psi_i^\dagger(\vec{x}) \vec{\alpha} \psi_i(\vec{x})\right) = \frac{R}{6} \frac{4RE_{kin,i} + 2m_i R - 3}{2RE_{kin,i}(RE_{kin,i} - 1) + m_i R}.$$

Where $E_{kin,i}$ is the kinetic energy of quark i. The function I in Eq. (2.28) is

$$I(m_i, m_j, R) = 1 + 2\int_0^R \frac{dr}{r^4} \mu(m_i, r) \mu(m_j, r).$$

The mean product of the spins $\langle \vec{\sigma}_i \vec{\sigma}_j \rangle$ is calculated in Appendix B.

Electric interaction

The effect of the electric interaction energy is comparably small. For example for the mesons whose masses will be calculated, it does not vanish only for the K and K^*, where $E_{el} \approx 4MeV$. Nevertheless, it is included in the total hadron mass. Eq. (2.25) integrates as:

$$E_{el} = -\frac{2\alpha_S}{3} \cdot \int_0^R dr \sum_{i>j} \left(\frac{\rho_i(r) - \rho_j(r)}{r}\right)^2. \tag{2.29}$$

Here $\rho_i(r)$ is the integral over the charge density of the i-th quark to a radius r: $\rho_i(r) = \int_0^r dr' 4\pi r'^2 \psi_i^\dagger(r') \psi_i(r')$.

2.2.4 Calculating the resulting mass

Now all the above calculations, Eqs. (2.20), (2.21), (2.28) and (2.29) are summarized together with the volume term $E_{vol} = V \cdot B$ as the mass of the hadron:

$$M(r) = \sum_{i=1}^{2,3} E_{kin,i}(r) + E_0(r) + E_{mag}(r) + E_{el}(r) + \frac{4\pi}{3} r^3 B.$$

Fig. 2.3 shows the $M(r)$ dependency for the Σ^+ baryon. As the plot shows, the mass has one well-behaved minimum. This minimum is $M(R)$ with

$$\left.\frac{\partial M}{\partial r}\right|_{r=R} \stackrel{!}{=} 0.$$

This minimum is generally found numerically, and used as the resulting mass. Only in the case where all constituent quarks are massless an analytic expression is possible.

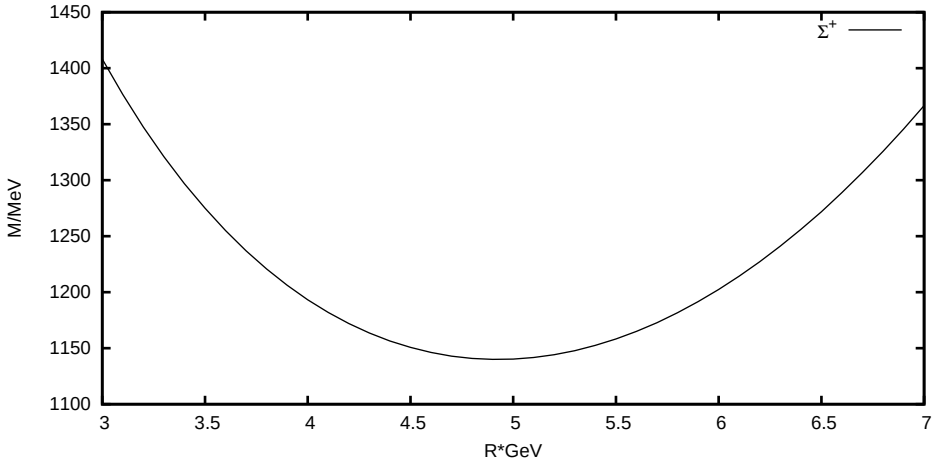

Figure 2.3: Mass over radius for the Σ^+. The minimum is at $R \approx 4.9$ GeV^{-1} and the mass becomes $M(R) \approx 1140$ MeV.

Massless quarks

The case becomes especially easy for massless quarks. Here, the boundary condition in Eq. (2.17) becomes independent of the quark energy. The first root now simply is $pR = 2.04$, and the kinetic energy becomes $E_{kin} = \frac{2.04}{R}$. The magnetic interaction energy is calculated as $E_{mag} = \frac{\lambda \langle \vec{\sigma}_i \vec{\sigma}_j \rangle \alpha_S \cdot 0.053}{R}$ and the electric interaction vanishes. In this case the minimization is easily done, and the mass becomes

$$M = \frac{A}{R} + \frac{4\pi}{3} R^3 B = \frac{4}{3} A^{3/4} (4\pi B)^{1/4}, \tag{2.30}$$

where $A = n \cdot 2.04 + \lambda \sum_{i>j}^{n} \langle \vec{\sigma}_i \vec{\sigma}_j \rangle \alpha_S \cdot 0.053 + Z_0$, with number of quarks n. A is a constant for each hadron.

2.3 Fitting the parameters

To fit B, Z_0 and α_S the N, Δ and ω hadrons are used. The quark masses are set to zero ($m_u = m_d = 0$). This yields $B^{1/4} = 146.2$ MeV, $Z_0 = -1.86$ and $\alpha_S = 2.19$. These

results are the same as in Ref. [3]. Then, the strange quark mass is fitted against the Ω^-, which yields $m_s = 277.7$ MeV. Similarly one would find the mass of the charm quark as $m_c = 1546.6$ MeV if fitted against the J/ψ. But because of their high masses, which are unimportant in the following thermodynamics, charmed hadrons won't be discussed here.

One comment is in order here: The coupling constant α_S is to large to justify a perturbative approach as it was done to calculate the interaction energies. Nevertheless, the results are quite good, and this problem is not investigated further.

2.4 The hadronic mass spectrum

2.4.1 Results for light hadrons

The resulting masses for hadrons consisting of u,d and s quarks are shown in Table 2.1, using the parameters of section 2.3. While most of the results are pretty good for such a naive model as the bag model, it is noticeable that the pion mass is two times to large.

Particle	M_{exp}	M_{bag}	E_{kin}	E_{mag}	E_{el}	E_0	E_{vol}	R
N	938	$938^{(*)}$	1234	-156	0	-374	235	4.968
Λ	1116	1100	1405	-158	1.35	-377	228	4.924
Σ^+	1189	1140	1405	-118	1.35	-377	229	4.926
Ξ^0	1321	1291	1598	-138	9.22	-382	221	4.867
Δ	1236	$1236^{(*)}$	1125	143	0	-341	309	5.446
Σ^*	1385	1381	1297	124	1.35	-344	302	5.406
Ξ^*	1533	1534	1470	108	9.82	-347	294	5.354
Ω^-	1672	$1672^{(*)}$	1640	93	0	-350	288	5.318
π	139	273	1241	-472	0	-564	68	3.293
ω/ρ	783	$783^{(*)}$	873	111	0	-397	196	4.677
K	495	488	1425	-424	3.37	-579	63	3.209
K^*	892	927	1043	92.1	4.45	-402	189	4.623
ϕ	1019	1065	1211	77.3	0	-406	183	4.575

Table 2.1: Spectrum of hadrons compared to experimental values taken from Ref. [7]. Masses/Energies are given in MeV, the radius in 1/GeV. The masses marked with a $^{(*)}$ are used for the fit.

2.4.2 Higher radial excitations

Until now only the smallest root of Eq. (2.17) has been used to determine the momentum of a quark. But the equation has infinite roots (becoming $\pi/2$-periodic for large arguments), what happens if those are used? These radial excited baryons share the same quantum numbers as the ground state. For example the nucleon $N(1440)$ shares its quantum numbers with the ground state $N(939)$. This hadron may be identified with a bag containing a radial excited quark. The first nucleon excitations are listed in Table 2.2. The known experimental values would be 1440 MeV, 1710 MeV and 2100 MeV, see Ref. [7]. As this example shows, the results from the bag model are to narrow in comparison to the experimental values. In Fig. 2.4 the mass density resulting of radial excitations is shown and compared to the mass density resulting from experimental data. In the figure all hadrons (including their degeneracy factors) in a given range are summarized. The comparison to the experimental values shows the same effect as in Table 2.2, the bag model leads to a

number of hadrons that is too large. The cubic fit shown in Fig. 2.4 is explained in the following section.

n_1	n_2	n_3	M_{bag}
2	1	1	1351
2	2	1	1601
3	1	1	1705
2	2	2	1890
3	2	1	1918

Table 2.2: Radial excitations of the nucleon. n_i denotes the number of root in the boundary condition.

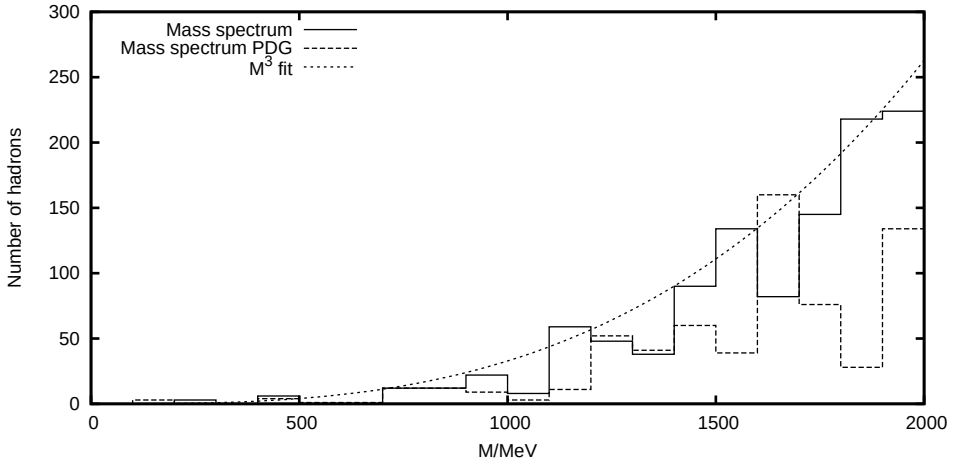

Figure 2.4: Histogram showing the mass density with a bin size of 100 MeV. The cubic fit shows a good agreement. As a comparison, the mass density taken from Ref. [7] with baryons up to 2000 MeV and mesons up to 1800 MeV is shown.

2.4.3 Asymptotic mass spectrum and Hagedorn temperature

In Ref. [6] R. Hagedorn introduced a maximum temperature above which the partition function of a hadronic gas would diverge. This happens if the density of hadrons grows exponentially. Taking the partition function for a high number of particles as

$$Z = \sum_k \int dm \rho(m) \exp\left[-\frac{H_k}{T}\right],$$

the divergence happens if the asymptotic density of particles $\rho(m)$ increases faster than $\exp(m/T_H)$. Then, the integrand for the ground state ($H = m$) becomes proportional to $\exp\left[m\left(\frac{1}{T_H} - \frac{1}{T}\right)\right]$. For $T \geq T_H$, the integral over m diverges. Therefore, the Hagedorn temperature T_H is the upper boundary for the temperature of a hadronic system. This means that all thermodynamical properties, which are derivatives of the partition function, also diverge.

The asymptotic mass spectrum for radial excited bags

With radial excitations as in section 2.4.2 the number of hadrons does not grow exponentially, which is now proven. In the following, hadrons consisting of massless quarks are investigated for simplicity. As stated above, for high arguments the boundary condiction becomes $\pi/2$-periodic. So the kinetic energy becomes $E_{kin} \approx \frac{\pi n}{2r}$, where n is the number of the root. The factor A in Eq. (2.30) now becomes approximately proportional to $N = n_1 + n_2 + n_3$ for baryons and $N = n_1 + n_2$ for mesons:

$$m \propto N^{3/4}.$$

The number of masses in an interval $[m, m+\Delta m]$ is therefore proportional to $(m+\Delta m)^{4/3} - m^{4/3}$. This number is degenerated: N can be composed in $\binom{N}{k}$ ways, where k is the number of quarks in the bag. For mesons the degeneracy is N and for baryons it is $N(N-1) \approx N^2$. With these the density function becomes

$$\rho(m) \propto \frac{(m+\Delta m)^{4/3} - m^{4/3}}{\Delta m} \binom{N}{k}.$$

Now the limes $\Delta m \to 0$ is built and N is expressed through m. The asymptotical density function for the MIT Bag Model becomes

$$\rho(m) \propto \begin{cases} m^{5/3}, & \text{for mesons} \\ m^3, & \text{for baryons} \end{cases}.$$

In Fig. 2.4 an m^3 fit shows a good agreement with the numerical results. The case is not different if one takes into account higher angular momenta (ignoring that the bags would not be spherical anymore), because the roots to the boundary condition would approximately grow linearly, giving a similar situation as with radial excitations. Therefore, the MIT Bag Model does not lead to a Hagedorn temperature.

Bags with growing numbers of quark-antiquark pairs

A way to get to a Hagedorn temperature is described for example in Ref. [1]. A high number of quark-antiquark pairs is introduced inside the bag. These pairs are treated as a non-interacting ideal gas. On one hand, in an ideal gas the pressure is related to the temperature through a Stefan-Boltzmann like law (see section 3.1):

$$p = \frac{g\pi^2}{90} T^4,$$

where g is the degeneracy factor, $8 \cdot 2 + \frac{7}{8} 3 \cdot 2 \cdot 2 \cdot 2 = 37$ for a (massless) quark-antiquark-gluon gas. On the other hand, the pressure of the bag is identified with the bag constant. Therefore, the temperature has to be a constant, too:

$$T_H = \left(\frac{90}{\pi^2 g} B \right)^{1/4}. \tag{2.31}$$

With a bag constant of $B^{1/4} = 146$ MeV, one gets $T_H \approx 103$ MeV. This value is of course to low for a Hagedorn temperature, as for example the critical temperature for the phase transition to a quark-gluon plasma is expected to be around 180 MeV.

3 Thermodynamics

In this chapter the characteristics of a hadronic system as a thermodynamic gas are investigated. The goal is to describe the phase transition from a hadronic gas to a quark-gluon plasma (QGP). The QGP is described here as an ideal gas, while two models are used for the hadronic phase:

- An ideal gas of point-like particles in section 3.1.
- The compressible bag model in section 3.2.

3.1 Hadronic phase and quark-gluon plasma as an ideal quantum gas

A first approximations to a system of hadrons and the QGP is an ideal (Bose/Fermi) quantum gas. The grand canonical potential for this system is (see for example Ref. [8]):

$$\ln Z = \eta g V \int \frac{d^3k}{(2\pi)^3} \ln\left\{1 + \eta \exp\left(-\beta(E-\mu)\right)\right\}.$$

Here, $\eta = +1/-1$ for bosons/fermions, $E = \sqrt{k^2+m^2}$ and g is the degeneracy factor. From this, all other thermodynamical properties can be derived.

3.1.1 Pressure and energy density

The pressure p and the energy density ϵ of an ideal gas are calculated as follows:

$$\begin{aligned} p &= \frac{1}{\beta}\frac{\partial}{\partial V}\ln Z \\ &= \frac{\eta g}{\beta}\int \frac{d^3k}{(2\pi)^3}\ln\left\{1+\eta\exp\left(-\beta(E-\mu)\right)\right\}, \qquad (3.1) \\ \epsilon = \frac{\langle E\rangle}{V} &= -\frac{1}{V}\frac{\partial}{\partial\beta}\ln Z \\ &= g\int\frac{d^3k}{(2\pi)^3}\frac{E-\mu}{e^{\beta(E-\mu)}+\eta}. \qquad (3.2) \end{aligned}$$

In the case of massless constituents the integrals can be evaluated. For a vanishing chemical potential pressure and energy density become a form like the Stefan-Boltzmann law. For bosons:

$$p_B = \frac{g\pi^2 T^4}{90}, \quad \epsilon_B = 3p_B, \qquad (3.3)$$

and for fermions:

$$p_F = \frac{7}{8}\frac{g\pi^2 T^4}{90}, \quad \epsilon_F = 3p_F. \tag{3.4}$$

To compare the case of an hadronic gas with the massless case, p/T^4, ϵ/T^4 and $(\epsilon - 3p)/T^4$ are plotted, see Figs. 3.5, 3.6 and 3.7. In Fig. 3.1 $(\epsilon - 3p)/T^4$ is compared to lattice QCD data, which were extracted from Ref. [9] by F. Karsch. Just as in Ref. [9], the ideal quantum gas is in good agreement with the lattice data for the hadronic phase which ends at $T_C \approx 170$ MeV in the Karsch data. But the gradient of the ideal gas is to low compared to the lattice data. The situation is even worse when the experimental particle masses are used. Therefore, the problem is the used model not the used hadron data. The particles used to create the figures in this chapter are:

- Gluons, up-, down- and strange- quarks for the QGP. The quark masses are the same as they were used to calculate the hadronic mass spectrum, see section 2.3.
- The hadronic phase consists of all the particles in section 2.4.1 and all their radial excitations up to 2000 MeV for baryons and 1800 MeV for mesons. These upper limits were used in the Karsch data, too.

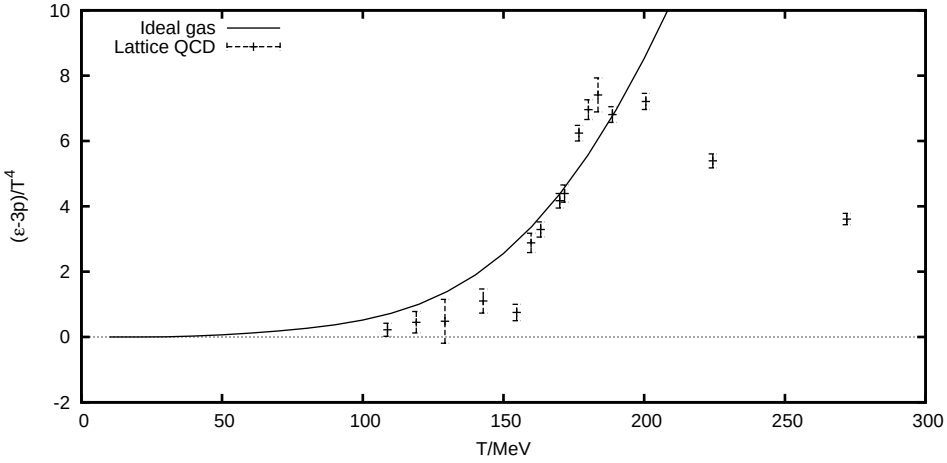

Figure 3.1: Comparison of $(\epsilon - 3p)/T^4$ for an ideal gas and lattice QCD data extracted from Ref. [9].

3.1.2 Critical temperature and phase diagram

The phase transition from a hadron gas to a quark-gluon plasma is characterized by the point where the pressure of the two phases become identical: $p_{hadron} = p_{qgp}$. Here, $p_{qgp} = \sum_{quarks} p_i + p_{gluon} - B$ is taken as an ideal gas. For the particle setup as above, the critical temperature becomes $T_C \approx 102$ MeV for $\mu = 0$, where B is the value from section 2.3. The critical baryo-chemical potential is about $\mu_C \approx 775$ MeV for $T = 0$. Fig. 3.3 shows the resulting phase diagram. The critical temperature can also be approximated by using that the pressure of the hadronic gas is much less than the bag constant at T_C and by treating the strange quark as massless. This gives

$$T_C \approx \left(\frac{90}{\pi^2 g} B\right)^{1/4}, \tag{3.5}$$

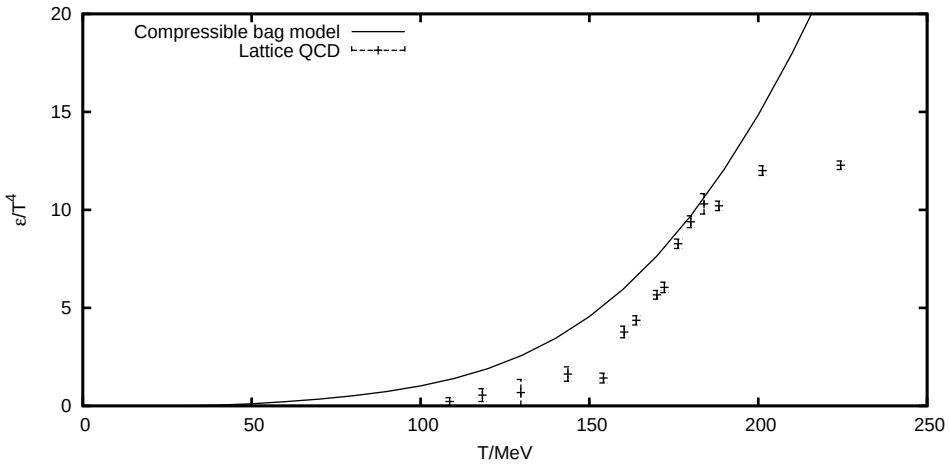

Figure 3.2: Comparison of the energy density for an ideal gas and lattice QCD data extracted from Ref. [9].

which is coincidental the same formula as Eq. (2.31). With a degeneracy factor of $8 \cdot 2 + \frac{7}{8} 3 \cdot 3 \cdot 2 \cdot 2 = 47.5$, including strange quarks, the critical temperature is approximated as 97 MeV. This is only 5 MeV below the value where the hadronic phase was included. For temperatures much larger than the particle masses, the pressure of the hadron gas becomes Stefan-Boltzmann-like, as in Eqs. (3.3) and (3.4). With a large number of hadrons the degeneracy factor also becomes large and exceeds the degeneracy factor of the quark-gluon plasma. So, the pressures for large temperatures are compared as $p_{hadron}/T^4 \propto g_{hadron} > p_{qgp}/T^4 \propto g_{qgp}$. This means that the pressure of the hadron gas will cross the pressure of the QGP again. This leads to a second phase transition to a second hadronic phase, which is shown in Fig. 3.3.

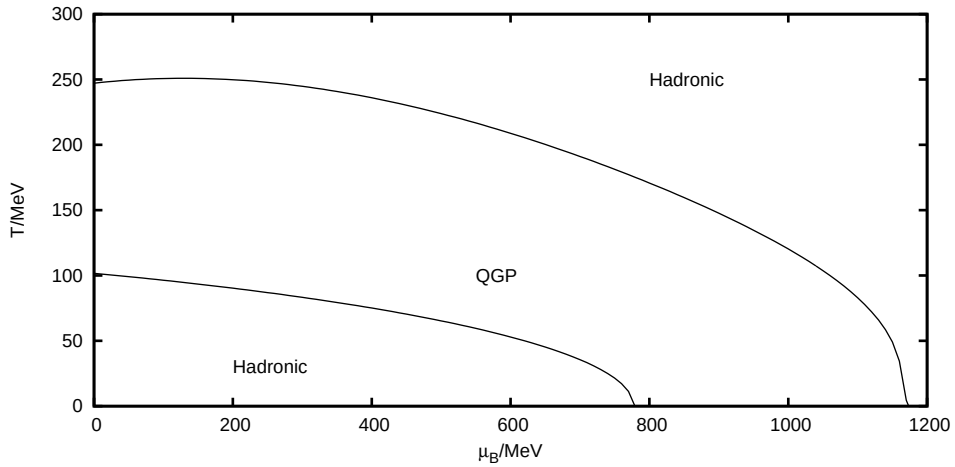

Figure 3.3: Phase diagram for an ideal quantum gas with an extra hadronic phase.

As shown above, two problems arise in the model of an ideal gas:

1. Depending on the number of hadrons in the gas the hadronic pressure may exceed the QGP pressure again. This unphysical behavior is corrected in the compressible bag model described in section 3.2. Fig. 3.5, showing the pressure at $\mu = 0$, illustrates what happens.

2. The critical temperature is expected to be around $170-190$ MeV, so the result above is much to low. This can be corrected by using a larger bag constant.

To solve the second problem, the bag constant has to be altered. To be consistent with chapter 2, the mass spectrum is altered, too: Using the N and Δ to fit Z_0 and α_S and the Ω^- to fit the strange mass, but keeping B as a free variable, gives rise to some slightly better results. While the critical temperature rises with the bag constant, the pion mass decreases. At $B^{1/4} = 181$ MeV m_π hits zero and T_C becomes 131 MeV. With a larger bag constant the pion mass becomes negative, so 131 MeV is the largest critical temperature that is possible within this model, as long as the masses of the N, Δ and Ω^- are taken as fixed values.

3.2 Compressible bag model

A modified model for the thermodynamical properties of a hadronic gas has been introduced in Ref. [10]. In the compressible bag model a Van-der-Waals like way of describing the gas is chosen, where the volume of the bags is subtracted from the volume of the system. Note that this can be considered a more realistic approach to a gas of MIT bags as they have a well-defined volume. The volume becomes

$$V' = V - b\sum_{i=1}^{n} N_i v_i, \tag{3.6}$$

where b is the exclusion efficiency parameter, N_i the number of particles of type i and v_i the volume of one such particle. The exclusion efficiency parameter will be chosen to scale the nucleon's bag radius to the proton charge radius. Now the free energy of the total system is written as:

$$\hat{F}(N, V', T) = \sum_{i=1}^{n} F_f(N_i, V', T, M_i(v_i)).$$

Where $F_f(N, V, T, M) = -p_f(\mu, T, M) \cdot V + \mu \cdot N$ is the free energy as in the free quantum gas discussed above. With the new volume in Eq. (3.6), the chemical potential μ has to be changed, and the free energy is $F_f(N, V', T, M) = -p_f(\mu', T, M) \cdot V' + \mu' \cdot N$. Now the requirement of the bag model, that the mass has to be minimized with respect to the volume, is replaced by the minimization of $\hat{F}$ with respect to v_i:

$$\frac{\partial \hat{F}}{\partial v_i} = N_i \left(bp + N_i^{-1} \frac{\partial F_f}{\partial M_i} \frac{\partial M_i}{\partial v_i} \right) \stackrel{!}{=} 0. \tag{3.7}$$

The term $N_i^{-1} \frac{\partial F_f}{\partial M_i}$ is equal to the mean inverse Lorentz factor $\langle \gamma^{-1} \rangle$:

$$N_i^{-1} \frac{\partial F_f}{\partial M_i} = \frac{-\frac{\partial p_f}{\partial M_i}}{\frac{\partial p_f}{\partial \mu'}} = \frac{\int \frac{d^3k}{(2\pi)^3} \frac{M_i}{E} \frac{1}{\exp((E-\mu')/T)+\eta_i}}{\int \frac{d^3k}{(2\pi)^3} \frac{1}{\exp((E-\mu')/T)+\eta_i}} = \left\langle \frac{M_i}{E} \right\rangle = \langle \gamma^{-1} \rangle . \tag{3.8}$$

The nonrelativistic case $\langle \gamma^{-1} \rangle \approx 1$ significantly decreases computation time, it will later be discussed where it applies. With Eq. (3.8) Eq. (3.7) becomes:

$$\frac{\partial M_i}{\partial v_i} = -\frac{bp}{\langle \gamma^{-1} \rangle}. \tag{3.9}$$

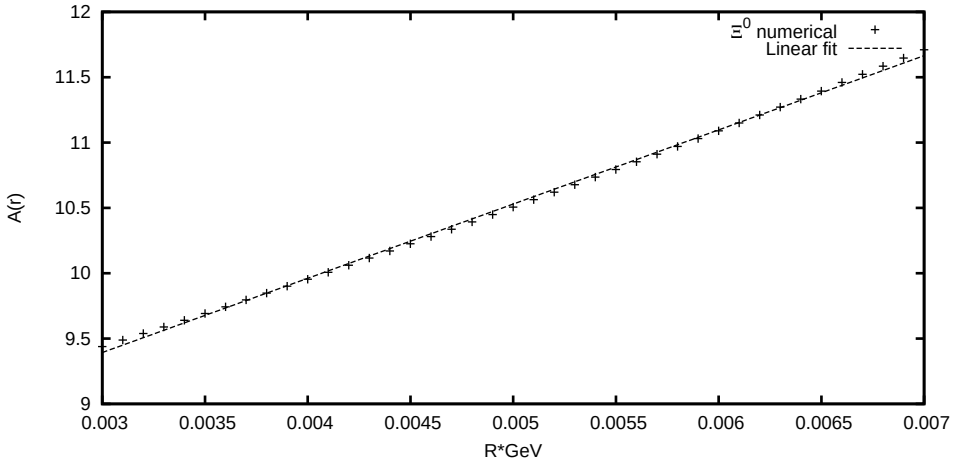

Figure 3.4: The function $A(r)$ for the Ξ^0 together with a linear fit.

This equation is equivalent to the bag model in vacuum for either $p = 0$ or $b = 0$, as one should expect. The extra pressure from the gas leads to a compression of the bags, which again leads to an increased mass of the bags. Recall the bag equation:

$$M_i(v_i) = \frac{A_i(v_i)}{v_i^{1/3}} + Bv_i, \tag{3.10}$$

written here as a function of the volume $v_i = \frac{4\pi}{3}R_i^3$. $A_i(v_i)$ is independent of the volume for massless quarks only, see section 2.2.4. From comparison with numerical results, a linear approximation $A(v) = A_0 + d \cdot v^{1/3}$ is very good. Fig. 3.4 shows an exemplary illustration of a linear fit to the function $A(r)$. A_0 will be eliminated by using the bag equation in vacuum and d will be computed with the techniques developed in chapter 2 for each hadron. The mass of the bag in vacuum is defined as m_i with $\frac{\partial m_i}{\partial v_i} = 0$, while the mass of the bag inside the gas is M_i. Using Eqs. (3.9) and (3.10), the problem is almost solved. It follows

$$v_i(p, m_i) = \frac{m_i - d_i}{4B}\left(1 + \frac{bp}{B\left\langle\gamma^{-1}\right\rangle}\right)^{-3/4}, \tag{3.11}$$

$$M_i(p, m_i) = (m_i - d_i)\left(1 + \frac{3bp}{4B\left\langle\gamma^{-1}\right\rangle}\right)\left(1 + \frac{bp}{B\left\langle\gamma^{-1}\right\rangle}\right)^{-3/4} + d_i. \tag{3.12}$$

To fit the exclusion efficiency parameter b to the proton charge radius R_P, the volume $v_{N,0} = \frac{m_N}{4B}$ of the bag for the proton in vacuum is taken. b becomes

$$b = \frac{\frac{4}{3}\pi R_P^3}{v_{N,0}} = \frac{16\pi R_P^3 B}{3m_N},$$

where m_N is the nucleon mass. With this fit the only parameter of the compressible bag model is fixed.

The chemical potential μ is not identical to μ' in the free energy. The dependency is given by

$$\mu_i = \frac{\partial \hat{F}}{\partial N_i} = \frac{\partial F_f}{\partial N_i} + bv_i p = \mu_i' + bv_i p, \tag{3.13}$$

with $\mu_i = a_i \mu_B$ and the baryo-chemical potential μ_B.

3.2.1 Pressure and energy density

The total pressure p follows from Eqs. (3.1), (3.11), (3.12) and (3.13):

$$p = \sum_{i=1}^{n} p_f(T, \mu', M_i). \tag{3.14}$$

The right side of Eq. (3.14) depends on p itself, therefore a numerical algorithm has to be used to solve this equation additionally to the numerical integration.

The energy density is given by

$$\epsilon = \frac{1}{V}\frac{\partial\left(\beta\hat{F}\right)}{\partial\beta} = \sum_{i=1}^{n}\left[\mu'\rho_i - \left(1 - b\sum_{i=1}^{n}\rho_i v_i\right) g\int \frac{d^3k}{(2\pi)^3}\frac{\mu' - E}{e^{\beta(E-\mu')}+\eta}\right],$$

with the particle density

$$\rho_i = \frac{\partial p_f}{\partial\mu} = g\int \frac{d^3k}{(2\pi)^3}\frac{1}{e^{\beta(E-\mu')}+\eta}.$$

The pressure and the energy density are shown in Figs. 3.5, 3.6 and 3.7, where they are compared to the ideal gas. For low temperatures (< 130 MeV) the compressible bag model resembles the ideal gas. This also includes that the critical temperature (which is below 130 MeV here) will not change significantly. But as the plot of the pressure shows, the second phase transition disappears. Pressure and energy density in the compressible bag model compare poorly to the lattice data, the ideal gas gives a better description of these values. This is in contrast to the phase diagram which is more realistic in the compressible bag model.

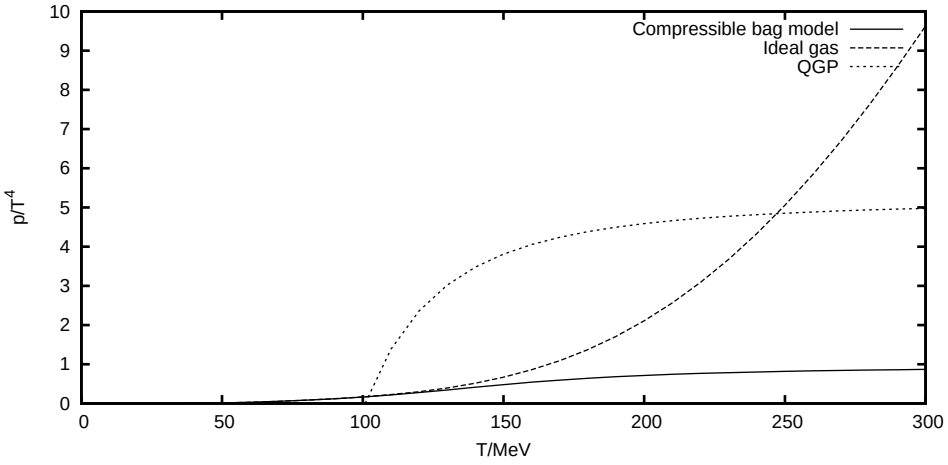

Figure 3.5: The pressure for the hadronic phase in both models and for the QGP phase. The figure nicely shows how the lowered pressure in the compressible bag model circumvents a second phase transition.

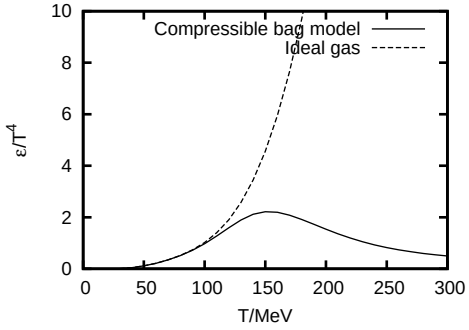

Figure 3.6: Energy density for compressible bags and an ideal gas.

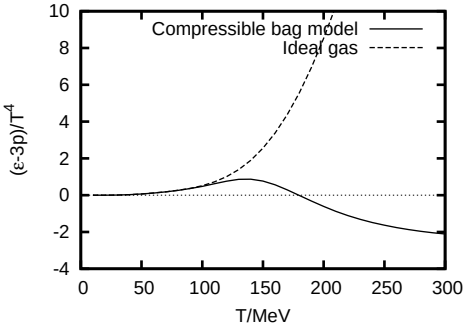

Figure 3.7: Comparison of energy density and pressure, $(\epsilon - 3p)/T^4$, for compressible bags and an ideal gas.

3.2.2 Phase diagram

The quark-gluon plasma is again taken as an ideal quantum gas, just as in section 3.1. The masses for the hadronic phase are also the same. The compressible bag model gives the expected result, with no additional hadronic phase, as shown in Fig. 3.8. Here, the approximation $\langle \gamma^{-1} \rangle \approx 1$ mentioned above is made, leading to a negligible error but decreasing computation time. For example, the pion pressure at 165 MeV is only 0.3 % to small in the nonrelativistic case.

The phase diagram in Fig. 3.8 still has two problems:

1. T_C still is too low for the bag constant used here.
2. The hadronic phase could well be approximated with $p_{had} = 0$ and would still lead to almost the same phase diagram. This is caused by the low hadronic pressure at T_C, as Fig. 3.5 shows.

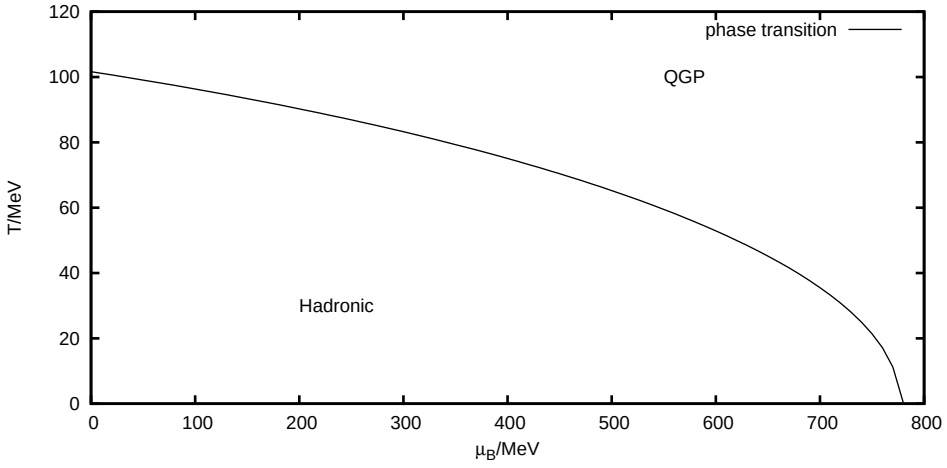

Figure 3.8: Phase diagram for the compressible bag model.

4 Summary

In the second chapter the MIT Bag Model has been investigated. On the level of the bag Lagrangian it has been found that the chiral symmetry is explicitly broken on the bag's surface. Nevertheless, the masses of nine hadrons have been predicted on basis of the masses of four hadrons as fit parameters. These predictions are good, considering the simplicity of the model. Only the mass of the pion is significantly to large, as it is twice the pion mass found experimentally. Hadrons with an excited angular momentum can not be treated in a theory of spherical bags. Radial excitations are possible, but give results which are too narrow. While the spectrum grows strongly it does not grow exponentially in the asymptotic case. Therefore, the MIT Bag Model does not predict a Hagedorn temperature without being modified.

In the third chapter the thermodynamics of a gas of bags has been investigated by using two models. These have been used to calculate the pressure, the energy density and a phase diagram to a quark-gluon plasma. The first model treats treats the gas of bags as a gas of ideal point-like particles. It gives a considerably good agreement with data from lattice QCD for the pressure and the energy density of the hadronic phase, while the phase diagram has two flaws: The critical temperature is too low a value and an extra hadronic phase appears for large temperatures and for large chemical potentials. In the second model, the bag volume has been incorporated in form of the compressible bag model. This leads to a more reasonably phase diagram with only one hadronic phase, and is in this regard a better model of a gas of bags. The downsides of the compressible bag model are that the problem of the low critical temperature has not been solved, and that pressure and energy density do not agree with the lattice data.

A Numerical calculations

All numerical calculations here were done with C++ programs using the GNU Scientific Library (GSL) and the GNU C Compiler (GCC). The used program versions were GCC 3.3.5 and GSL 1.6. The GSL has been used mainly for numerical integration on infinite intervals, a root finding algorithm and the spherical Bessel functions. For numerical integration the function `gsl_integration_qagiu` with a relative error of 10^{-5} has been used. For root finding it was Brent's method with a relative error of 10^{-4} and a maximum of 100 iterations.

B Spin-Spin coupling

For the magnetic interaction energy the mean product of the spins of two quarks, $\langle \vec{\sigma}_1 \cdot \vec{\sigma}_2 \rangle$, has to be calculated in dependency of the total angular momentum $\vec{J}$. The angular momentums $\vec{l}$ of the quarks are zero in the MIT Bag Model. For a meson this is easy by squaring $\vec{J} = \vec{s}_1 + \vec{s}_2$: $\vec{\sigma}_1 \vec{\sigma}_2 = 4 \cdot \left(\frac{1}{2} J(J+1) - \frac{3}{4}\right)$. For a baryon, the wave functions coupling to a total Spin J have to be found explicitly. The operator $\vec{\sigma}_i \cdot \vec{\sigma}_j$ can be represented by $T_{i,j} - 1$, where $T_{i,j}$ switches the z-component of the quarks i and j. For the wave functions first quarks two and three are coupled to a total spin $J_{23} \in \{1, 0\}$. Then, quark one is coupled against spin J_{23} to a total spin $J \in \{\frac{3}{2}, \frac{1}{2}\}$. Note that the result is independent of J_z. The results are given in Table B.1.

	$J = 3/2$	$J = 1/2$	
	$J_{23} = 1$	$J_{23} = 1$	$J_{23} = 0$
$\langle \vec{\sigma}_1 \cdot \vec{\sigma}_2 \rangle$	1	1	-3
$\langle \vec{\sigma}_1 \cdot \vec{\sigma}_3 \rangle$	1	-2	0
$\langle \vec{\sigma}_2 \cdot \vec{\sigma}_3 \rangle$	1	-2	0

Table B.1: Spin products for a baryon.

Bibliography

[1] R. K. Bhaduri, "MODELS OF THE NUCLEON: FROM QUARKS TO SOLITON," *REDWOOD CITY, USA: ADDISON-WESLEY (1988) 360 P. (LECTURE NOTES AND SUPPLEMENTS IN PHYSICS, 22)*

[2] A. Chodos, R. L. Jaffe, K. Johnson, C. B. Thorn and V. F. Weisskopf, "A New Extended Model Of Hadrons," Phys. Rev. D **9** (1974) 3471.

[3] T. A. DeGrand, R. L. Jaffe, K. Johnson and J. E. Kiskis, "Masses And Other Parameters Of The Light Hadrons," Phys. Rev. D **12** (1975) 2060.

[4] F. Schwabl, "Quantenmechanik für Fortgeschrittene: QM II," *Springer, Berlin Heidelberg, 1997*

[5] C.W. Wong, "Center-of-mass correction in the MIT bag model," Phys. Rev. D **24** (1981) 1416.

[6] R. Hagedorn, "Statistical thermodynamics of strong interactions at high-energies," Nuovo Cim. Suppl. **3** (1965) 147.

[7] W. M. Yao *et al.* [Particle Data Group], "Review of particle physics," J. Phys. G **33** (2006) 1.

[8] F. Schwabl, "Statistische Mechanik," *Springer, Berlin Heidelberg, 2006*

[9] F. Karsch, K. Redlich and A. Tawfik, "Hadron resonance mass spectrum and lattice QCD thermodynamics," Eur. Phys. J. C **29** (2003) 549 [arXiv:hep-ph/0303108].

[10] S. Kagiyama, A. Nakamura and T. Omodaka, "A COMPRESSIBLE BAG MODEL EQUATION OF STATE AND SUBMILLISECOND PULSAR IN SN1987A,"